

## RESEARCH ARTICLE

# Replication study of plasma proteins relating to Alzheimer's pathology

Liu Shi<sup>1</sup> | Laura M. Winchester<sup>1</sup> | Sarah Westwood<sup>1</sup> | Alison L. Baird<sup>1</sup> |  
 Sneha N. Anand<sup>1</sup> | Noel J Buckley<sup>1</sup> | Abdul Hye<sup>2</sup> | Nicholas J. Ashton<sup>2,3,4</sup> |  
 Isabelle Bos<sup>5,6</sup> | Stephanie J. B. Vos<sup>5</sup> | Mara ten Kate<sup>6</sup> | Philip Scheltens<sup>6</sup> |  
 Charlotte E. Teunissen<sup>7</sup> | Rik Vandenberghe<sup>8</sup> | Silvy Gabel<sup>8,9</sup> | Karen Meersmans<sup>8,9</sup> |  
 Sebastiaan Engelborghs<sup>10,11</sup> | Ellen E. De Roeck<sup>10,12</sup> | Kristel Slegers<sup>13,14</sup> |  
 Giovanni B. Frisoni<sup>15,16</sup> | Olivier Blin<sup>17</sup> | Jill C. Richardson<sup>18</sup> | Régis Bordet<sup>19</sup> |  
 José L. Molinuevo<sup>20,21</sup> | Lorena Rami<sup>21</sup> | Anders Wallin<sup>22</sup> | Petronella Kettunen<sup>22</sup> |  
 Magda Tsolaki<sup>23</sup> | Frans Verhey<sup>5</sup> | Alberto Lléo<sup>24</sup> | Isabel Sala<sup>25</sup> | Julius Popp<sup>26,27</sup> |  
 Gwendoline Peyratout<sup>26</sup> | Pablo Martinez-Lage<sup>28</sup> | Mikel Tainta<sup>28</sup> |  
 Peter Johannsen<sup>29</sup> | Yvonne Freund-Levi<sup>2,30</sup> | Lutz Frölich<sup>31</sup> | Valerija Dobricic<sup>32</sup> |  
 Cristina Legido-Quigley<sup>33,34</sup> | Frederik Barkhof<sup>35,36</sup> | Ulf Andreasson<sup>3,37</sup> |  
 Kaj Blennow<sup>3,37</sup> | Henrik Zetterberg<sup>3,37,38,39</sup> | Johannes Streffer<sup>13,40</sup> |  
 Christina M. Lill<sup>41,42</sup> | Lars Bertram<sup>32,43</sup> | Pieter Jelle Visser<sup>5,6</sup> | Hartmuth C. Kolb<sup>44</sup> |  
 Vaibhav A. Narayan<sup>44</sup> | Simon Lovestone<sup>1,44</sup> | Alejo J. Nevado-Holgado<sup>1</sup>

<sup>1</sup> Department of Psychiatry, University of Oxford, Oxford, UK

<sup>2</sup> Maurice Wohl Clinical Neuroscience, Institute of Psychiatry, Psychology and Neuroscience, Kings College London, London, UK

<sup>3</sup> Department of Psychiatry and Neurochemistry, the Sahlgrenska Academy at the University of Gothenburg, Mölndal, Sweden

<sup>4</sup> Wallenberg Centre for Molecular and Translational Medicine, University of Gothenburg, Gothenburg, Sweden

<sup>5</sup> Department of Psychiatry and Neuropsychology, School for Mental Health and Neuroscience, Alzheimer Centrum Limburg, Maastricht University, Maastricht, the Netherlands

<sup>6</sup> Alzheimer Center, VU University Medical Center, Amsterdam, the Netherlands

<sup>7</sup> Neurochemistry lab, Department of Clinical Chemistry, Amsterdam University Medical Centers, Vrije Universiteit, Amsterdam Neuroscience, Amsterdam, the Netherlands

<sup>8</sup> University Hospital Leuven, Leuven, Belgium

<sup>9</sup> Laboratory for Cognitive Neurology, Department of Neurosciences, KU Leuven, Leuven, Belgium

<sup>10</sup> Reference Center for Biological Markers of Dementia (BIODEM), Institute Born-Bunge, University of Antwerp, Antwerp, Belgium

<sup>11</sup> Department of Neurology, UZ Brussel and Center for Neurosciences (C4N), Vrije Universiteit Brussel, Brussels, Belgium

<sup>12</sup> Department of Neurology and Memory Clinic, Hospital Network Antwerp (ZNA) Middelheim and Hoge Beuken, Antwerp, Belgium

<sup>13</sup> Complex Genetics Group, VIB Center for Molecular Neurology, VIB, Antwerp, Belgium

<sup>14</sup> Institute Born-Bunge, Department of Biomedical Sciences, University of Antwerp, Antwerp, Belgium

<sup>15</sup> University of Geneva, Geneva, Switzerland

<sup>16</sup> IRCCS Istituto Centro San Giovanni di Dio Fatebenefratelli, Brescia, Italy

<sup>17</sup> Aix marseille university, INS, Ap-hm, Marseille, France

<sup>18</sup> Neurosciences Therapeutic Area, GlaxoSmithKline R&D, Stevenage, UK

This is an open access article under the terms of the [Creative Commons Attribution-NonCommercial-NoDerivs](https://creativecommons.org/licenses/by-nc-nd/4.0/) License, which permits use and distribution in any medium, provided the original work is properly cited, the use is non-commercial and no modifications or adaptations are made.

© 2021 The Authors. *Alzheimer's & Dementia* published by Wiley Periodicals LLC on behalf of Alzheimer's Association

- <sup>19</sup> Inserm, University of Lille, CHU Lille, Lille, France
- <sup>20</sup> Alzheimer's Disease and Other Cognitive Disorders Unit, Hospital Clínic-IDIBAPS, Barcelona, Spain
- <sup>21</sup> Barcelona Beta Brain Research Center, Universitat Pompeu Fabra, Barcelona, Spain
- <sup>22</sup> Institute of Neuroscience and Physiology, Sahlgrenska Academy at University of Gothenburg, Gothenburg, Sweden
- <sup>23</sup> 1st Department of Neurology, AHEPA University Hospital, Makedonia, Thessaloniki, Greece
- <sup>24</sup> Hospital de la Santa Creu i Sant Pau, Barcelona, Spain
- <sup>25</sup> Department of Neurology, Hospital de la Santa Creu i Sant Pau, Barcelona, Spain
- <sup>26</sup> University Hospital of Lausanne, Lausanne, Switzerland
- <sup>27</sup> Geriatric Psychiatry, Department of Mental Health and Psychiatry, Geneva University Hospitals, Geneva, Switzerland
- <sup>28</sup> CITA-Alzheimer Foundation, San Sebastian, Spain
- <sup>29</sup> Danish Dementia Research Centre, Rigshospitalet, Copenhagen University Hospital, Copenhagen, Denmark
- <sup>30</sup> Karolinska Institutet Center for Alzheimer Research, Division of Clinical Geriatrics, School of Medical Sciences Örebro University and Department of Neurobiology, Caring Sciences and Society (NVS), Stockholm, Sweden
- <sup>31</sup> Department of Geriatric Psychiatry, Zentralinstitut für Seelische Gesundheit, University of Heidelberg, Mannheim, Germany
- <sup>32</sup> Lübeck Interdisciplinary Platform for Genome Analytics, Institutes of Neurogenetics and Cardiogenetics, University of Lübeck, Lübeck, Germany
- <sup>33</sup> Kings College London, London, UK
- <sup>34</sup> The Systems Medicine Group, Steno Diabetes Center, Gentofte, Denmark
- <sup>35</sup> Department of Radiology and Nuclear Medicine, VU University Medical Center, Amsterdam, the Netherland
- <sup>36</sup> UCL Institutes of Neurology and Healthcare Engineering, London, UK
- <sup>37</sup> Clinical Neurochemistry Laboratory, Sahlgrenska University Hospital, Mölndal, Sweden
- <sup>38</sup> UK Dementia Research Institute at UCL, London, UK
- <sup>39</sup> Department of Neurodegenerative Disease, UCL Institute of Neurology, London, UK
- <sup>40</sup> UCB, Braine-l'Alleud, Belgium, formerly Janssen R&D, LLC Beerse, Beerse, Belgium
- <sup>41</sup> Section for Translational Surgical Oncology and Biobanking, Department of Surgery, University of Lübeck and University Medical Center Schleswig-Holstein, Campus Lübeck, Lübeck, Germany
- <sup>42</sup> Ageing Epidemiology Research Unit, School of Public Health, Imperial College, London, UK
- <sup>43</sup> Department of Psychology, University of Oslo, Oslo, Norway
- <sup>44</sup> Janssen R&D, Beerse, UK

#### Correspondence

Liu Shi, Department of Psychiatry, University of Oxford, Oxford, UK.  
E-mail: [liu.shi@psych.ox.ac.uk](mailto:liu.shi@psych.ox.ac.uk)

#### Funding information

Innovative Medicines Initiative Joint Undertaking, Grant/Award Number: n° 115372; European Union's Seventh Framework Programme, Grant/Award Number: FP7/2007-2013; European Commission within the 5th framework program, Grant/Award Numbers: QLRT-2001-2455, #37670; Stichting voor Alzheimer Onderzoek, Grant/Award Numbers: #11020, #13007, #15005; Department of Health of the Basque Government, Grant/Award Number: 17.0.1.08.12.0000.2.454.01.41142.001.H; University of Antwerp Research Fund; Vetenskapsrådet, Grant/Award Number: #2018-02532; H2020 European Research Council, Grant/Award Number: #681712; Swedish State Support for Clinical Research, Grant/Award Number: #ALFGBG-720931; UK Dementia Research Institute

#### Abstract

**Introduction:** This study sought to discover and replicate plasma proteomic biomarkers relating to Alzheimer's disease (AD) including both the "ATN" (amyloid/tau/neurodegeneration) diagnostic framework and clinical diagnosis.

**Methods:** Plasma proteins from 972 subjects (372 controls, 409 mild cognitive impairment [MCI], and 191 AD) were measured using both SOMAscan and targeted assays, including 4001 and 25 proteins, respectively.

**Results:** Protein co-expression network analysis of SOMAscan data revealed the relation between proteins and "N" varied across different neurodegeneration markers, indicating that the ATN variants are not interchangeable. Using hub proteins, age, and apolipoprotein E  $\epsilon$ 4 genotype discriminated AD from controls with an area under the curve (AUC) of 0.81 and MCI convertors from non-convertors with an AUC of 0.74. Targeted assays replicated the relation of four proteins with the ATN framework and clinical diagnosis.

**Discussion:** Our study suggests that blood proteins can predict the presence of AD pathology as measured in the ATN framework as well as clinical diagnosis.

#### KEYWORDS

Alzheimer's disease, ATN framework, biomarker, dementia, network analysis, plasma proteomics, replication

## 1 | INTRODUCTION

Alzheimer's disease (AD) is characterized by the presence of amyloid beta ( $A\beta$ ) containing plaques and neurofibrillary tangles composed of modified tau protein together with the progressive loss of synapses and neurons.<sup>1</sup> Currently, the best characterized methods for measuring amyloid or tau pathology are positron emission tomography (PET) imaging and cerebrospinal fluid (CSF) measurement.<sup>2,3</sup> The National Institute on Aging and Alzheimer's Association (NIA-AA) have proposed a biomarker-based framework for classifying AD based on biomarkers of amyloid pathology (A), tau pathology (T), and neurodegeneration (N).<sup>4</sup> Briefly, "A" is measured by cortical amyloid PET ligand binding or CSF  $A\beta_{42}$ ; "T" is measured by CSF phosphorylated tau (p-tau) or cortical tau PET ligand binding; and "N" is by CSF total tau (t-tau), 18F-fluorodeoxyglucose (FDG) PET, or brain atrophy on magnetic resonance imaging (MRI). CSF neurofilament light chain (NfL) and neurogranin (Ng) may also be potential "N" markers.<sup>5,6</sup>

However, many of these measures are challenging because of their invasiveness, high cost, and limited availability.<sup>7,8</sup> Blood-based biomarkers show promise as a less invasive and potentially cost-effective option for the detection, classification, and monitoring of AD pathology. We have been seeking to develop multiplexed assays suitable for large-scale research screening using two approaches. In the first, we have used a range of mass-spectrometry proteomic approaches to generate a panel of "targeted proteins" to be used on multiplexed platforms; in the second we have used a proprietary near-proteomic wide aptamer capture array (SOMAscan).<sup>9–13</sup> Recently, we applied these approaches independently to the EMIF-AD Multimodal Biomarker Discovery study (EMIF-AD MBD), specifically in relation to the detection of amyloid.<sup>14,15</sup> Here, we develop this approach further, now combining both targeted and untargeted proteomics and using protein co-expression analysis and differential expression analysis to investigate changes in networks of proteins as well as individual proteins relating to the ATN framework (Figure 1). We have two objectives: first, to compare plasma protein profiles in a variety of ATN variants (using different "N" biomarkers) and second to test the replication of blood biomarkers relating to the ATN framework as well as to clinical phenotypes.

## 2 | METHODS

### 2.1 | Participants: EMIF-AD MBD study

The EMIF-AD MBD study is part of the European Medical Information Framework for AD (EMIF; <http://www.emif.eu/emif-ad-2/>); a public-private partnership funded through the Innovative Medicines Initiative (IMI). The design of the EMIF-AD MBD study has been described previously<sup>16</sup> but in brief,  $\approx$ 1200 samples from three groups of people (cognitively normal controls [CTL], mild cognitive impairment [MCI], and AD) were chosen from pre-existing cohorts with the goal of including samples from people with pathology as well as those without. All participating centers have agreed to share data as part of the EMIF-AD

### RESEARCH IN CONTEXT

- 1. Systematic review:** Plasma proteins are studied as candidate biomarkers to predict the "ATN" (amyloid/tau/neurodegeneration) diagnostic framework, while most such studies include small samples. Furthermore, few studies compare the difference between different ATN variants from the perspective of plasma proteins.
- 2. Interpretation:** Our findings offer new insights into changes in individual proteins and protein networks linked to various AD pathology markers as well as the ATN framework, particularly in preclinical stages of AD. Our results also indicate that ATN variants are not interchangeable because the relation between proteins and "N" vary across different neurodegeneration markers. Our study is the largest plasma proteomic study of various AD pathology markers, particularly the ATN framework, to our knowledge.
- 3. Future directions:** This work suggests that blood proteins can predict the presence of Alzheimer's disease (AD) pathology as measured in the ATN framework. Those nominated proteins are tractable targets for further mechanistic studies of AD pathology.

MBD study. Plasma was available on 972 subjects comprising 372 CTL, 409 MCI, and 191 AD. Samples were collected from the constituent cohorts in EMIF-AD using a range of protocols. General clinical and demographic information were available for all subjects (including apolipoprotein E [APOE]  $\epsilon$ 4 genotype data). In addition, each subject had a measure of brain amyloid load, using either CSF  $A\beta$  or amyloid PET. Furthermore, CSF t-tau and p-tau analysis data were available for more than 90% of the subjects. The classification of the status (abnormal/normal) of amyloid, t-tau, and p-tau has been described previously.<sup>16</sup>

In addition, the following AD-related phenotypes were also measured for the majority of the subjects (Table 1): (1) CSF NfL, Ng, and YKL-40; (2) MRI measures of hippocampal volume, cortical thickness, and white matter hyperintensities (WMH); (3) clinical assessments including baseline diagnosis, baseline Mini-Mental State Examination (MMSE) score, and MCI conversion.<sup>16</sup> The status (abnormal/normal) of NfL and hippocampal volume were determined by the median value of each marker within the whole data set.

We defined the ATN status for each participant using the above measurements. Briefly, we used CSF (or where not available, PET) amyloid as "A" and CSF p-tau181 as "T." For "N," we used CSF t-tau, NfL, and hippocampal volume as biomarkers of N. We then dichotomized these biomarkers as normal or abnormal and categorized them into four groups: no pathology (A-T-N-, referring as "A-TN-"), amyloid positive but both T and N negative (A+T-N-, referring as "A+TN-"), amyloid positive and T/N positive (including A+T-N+, A+T+N-, and

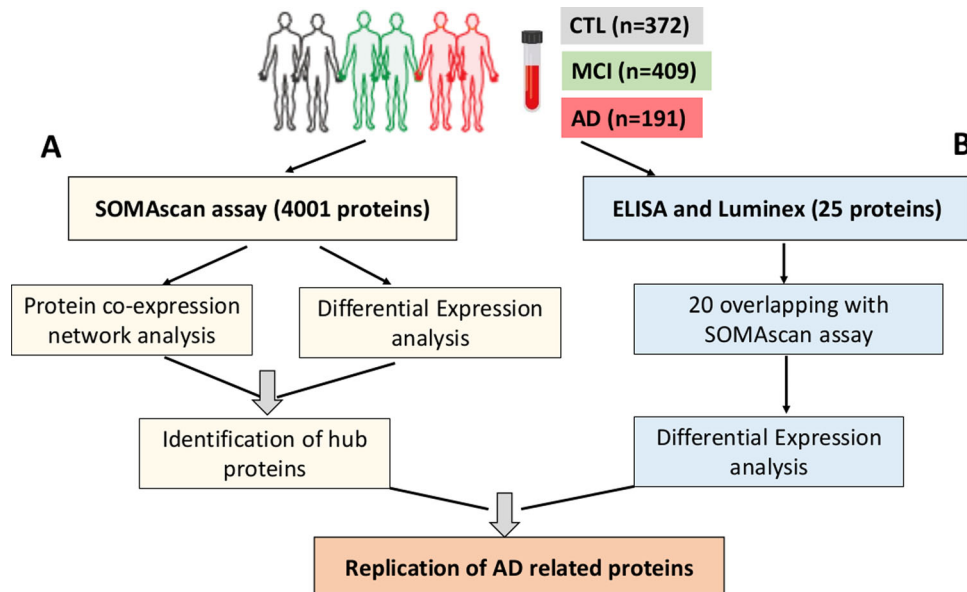


**FIGURE 1** Flowchart of study design. A, Measurement and quantification of 4001 proteins using SOMAscan assay; (B) Measurement and quantification of 25 proteins using enzyme-linked immunosorbent assay and Luminex. Twenty proteins overlapped between approach (A) and (B)

**TABLE 1** Demographics of EMIF participants included in the analysis by diagnosis. Percentage of cases is shown in brackets for male sex, APOE  $\epsilon 4$  carriers and the abnormality of amyloid, p-tau, and t-tau

| Characteristics                            | Sample size | CTL            | MCI             | AD              | P     |
|--|-------------|----------------|-----------------|-----------------|-------|
| N  | 972         | 372            | 409             | 191             | NA    |
| Age mean (SD), y                           | 972         | 64.6 (8.0)     | 69.9 (8.0)      | 70.5 (8.8)      | <.001 |
| Male sex N (%)                             | 972         | 209 (56)       | 216 (53)        | 103 (54)        | .64   |
| APOE $\epsilon 4$ + N (%)                  | 972         | 139 (37)       | 195 (48)        | 116 (61)        | <.001 |
| MMSE (SD)                                  | 967         | 28.8 (1.2)     | 26.2 (2.6)      | 21.4 (4.7)      | <.001 |
| Education mean (SD), y                     | 972         | 12.8 (3.7)     | 11.0 (3.7)      | 10.3 (3.9)      | <.001 |
| Amyloid + N (%)                            | 972         | 112 (30)       | 254 (62)        | 168 (88)        | <.001 |
| P-tau + N (%)                              | 876         | 53 (19)        | 215 (53)        | 128 (67)        | <.001 |
| T-tau + N (%)                              | 880         | 54 (19)        | 235 (58)        | 152 (80)        | <.001 |
| CSF NfL (SD) (pg/mL)                       | 643         | 742.1 (486.6)  | 1231.9 (2309.0) | 1777.6 (2843.1) | <.001 |
| CSF Ng (SD) (pg/mL)                        | 598         | 125.8 (203.9)  | 151.3 (199.1)   | 149.4 (125.3)   | .33   |
| CSF YKL-40 (SD) (ng/mL)                    | 649         | 141.9 (57.0)   | 176.9 (62.1)    | 191.4 (69.6)    | <.001 |
| Hippocampal volume (SD) in mm <sup>3</sup> | 633         | 7628.6 (883.7) | 6780.2 (1233.9) | 6220.2 (940.1)  | <.001 |
| Cortical thickness (SD) in mm              | 586         | 2.3 (0.1)      | 2.3 (0.1)       | 2.3 (0.1)       | .36   |
| WMH (SD) in mL                             | 617         | 0.9 (0.7)      | 1.1 (0.8)       | 1.0 (0.9)       | .02   |

Abbreviations: +, abnormality; AD, Alzheimer's disease; APOE, apolipoprotein E; CSF, cerebrospinal fluid; CTL, cognitively normal controls; MCI, mild cognitive impairment; MMSE, Mini-Mental State Examination; NfL, neurofilament light chain; Ng, neurogranin; p-tau, phosphorylated tau; SD, standard deviation; t-tau, total tau; WMH, white matter hyperintensities.

A+T+N+, referring as "A+TN+"), and suspected non-Alzheimer's pathology (SNAP, including A-T-N+, A-T+N-, and A-T+N+).

## 2.2 | Plasma analyses

We used two approaches to measure proteins in plasma samples collected from pre-existing cohorts as part of EMIF-AD MBD. First, we used the SOMAscan assay platform (SomaLogic Inc.) to measure pro-

teins in plasma. SOMAscan is an aptamer-based assay allowing for the simultaneous measurement and quantification of, in the version used here, 4001 proteins. The assay uses chemically modified nucleotides to transform a protein signal into a nucleotide signal that can be quantified using relative fluorescence on microarrays.<sup>17</sup> The abundance of each protein was log-transformed for all subsequent analyses. Second, we used enzyme-linked immunosorbent assay (ELISA) and Luminex xMAP assays to measure 25 proteins in the same subjects, as described previously.<sup>15</sup> Overall, 20 proteins overlapped between the

SOMAScan array and the second approach (ELISA and Luminex xMAP; Figure 1).

## 2.3 | Statistical analysis

All statistical analyses were completed using R (version 3.3.2). To compare baseline cohort characteristics across three different diagnostic groups (CTL, MCI, and AD), we used one-way analysis of variance (ANOVA) and chi-square tests to compare continuous and binary variables, respectively.

### 2.3.1 | Weighted gene correlation network analysis (WGCNA)

The R package WGCNA<sup>18</sup> was used to construct a co-expression network from the proteins obtained from the SOMAScan assay. This clustering is based on calculating correlations between paired variables, soft-threshold transforming them with a power function (i.e.,  $cor^\beta$ ), and using the result as an adjacency matrix between variables. The final step applies hierarchical clustering to this adjacency matrix. We applied this algorithm with default parameters, except for the following settings: soft threshold power  $\beta = 4$ , minimum module size = 10 proteins, merge cut height = 0.2. The resulting nine modules or groups of co-expressed proteins were used to calculate module eigenproteins. The eigenprotein-based connectivity (kME) was used to represent the strength of a protein's correlation with other protein module members. Proteins with high intramodular kME in the top 90th percentile within a module were considered hub proteins.

The correlation between eigenproteins and AD phenotypes was calculated, the *P* values were corrected with false discovery rate (FDR), and corrected *P* values were presented in a heat map. Furthermore, we used Student's *t*-test to assess pairwise difference of eigenproteins among different ATN framework and AD diagnostic groups as well as between MCI participants who subsequently converted to dementia (MCIc) within 3 years relative to those whose MCI remained stable (MCIs).

### 2.3.2 | Protein differential expression analysis

To compare the association of proteins with the ATN framework, we used logistic regression to compare proteins in different ATN profiles to "no pathology controls" (A-TN-), adjusting for age and APOE  $\epsilon 4$  genotype. *P* values were corrected using FDR and presented in volcano plots. To compare the replication of overlapping proteins in different ATN framework and AD diagnostic groups, we used Student's *t*-test to assess pairwise difference and presented *P* values in the box plots.

### 2.3.3 | Pathway enrichment analysis

Differentially expressed (DE) proteins and proteins within different modules were further nominated for pathway analysis using

WebGestalt software (<http://www.webgestalt.org/>). Briefly, DE proteins or proteins within a module were assembled into a "protein list" and all 4001 proteins measured by the SOMAScan assay were used as "background." This enrichment analysis was performed on the Kyoto Encyclopedia of Genes and Genomes database.

### 2.3.4 | Machine learning

Machine learning was used to identify optimal multivariate signatures, including both proteins and demographic data (age, sex, and APOE  $\epsilon 4$ ) as input features, to differentiate AD from CTL, and MCIc from MCIs. The classifier consisted of a two-stage approach (feature selection and classifiers) as described previously.<sup>14</sup> Briefly, Lasso was used to select the "n" top input features that best differentiated AD diagnostic groups. Support vector machine (SVM) classifiers were then built on top of these "n" features to predict the outcome under 10-fold cross-validation. For each analysis, the two steps (feature selection and classifiers) were performed over 100 iterations, where, in each iteration, the algorithm was allowed to use one feature more than in the previous iteration, starting with 1 feature and finishing with 100. Feature selection resulted in a list of features ranked by their correlation with AD diagnosis, of which the top "n" was selected for subsequent analysis. The classifier step was performed using the selected features to obtain a model to discriminate AD diagnosis. Those features that produced best performance were reported.

## 3 | RESULTS

### 3.1 | Subject demographics

Demographic information of subjects is shown in Table 1. No significant difference was observed in the distribution of sex. The CTL group was younger and had a lower proportion of APOE  $\epsilon 4$  carriers compared to the MCI and AD groups. Furthermore, the CTL participants had more years of education and higher MMSE scores. In terms of AD pathology markers, the ratio of abnormality of amyloid, p-tau, and t-tau in AD and MCI individuals was, as expected, significantly higher than in controls. Moreover, CSF NfL and YKL-40 were also significantly higher in AD and MCI while no difference was observed for CSF Ng across three different diagnostic groups. The MCI and AD groups had more hippocampal atrophy and more WMH than the CTL group.

### 3.2 | Plasma protein co-expression network analysis reveals modules linked to AD pathology markers

We first performed a network-based analysis of the plasma proteome as reported by the SOMAScan assay using WGCNA. We found nine modules (M) of co-expressed proteins and ranked them based on size from largest (M1;  $n = 1472$  proteins) to smallest (M9;  $n = 11$  proteins; Table S1 in supporting information). Figure 2A shows the clustering of these modules' concordance according to similarities in



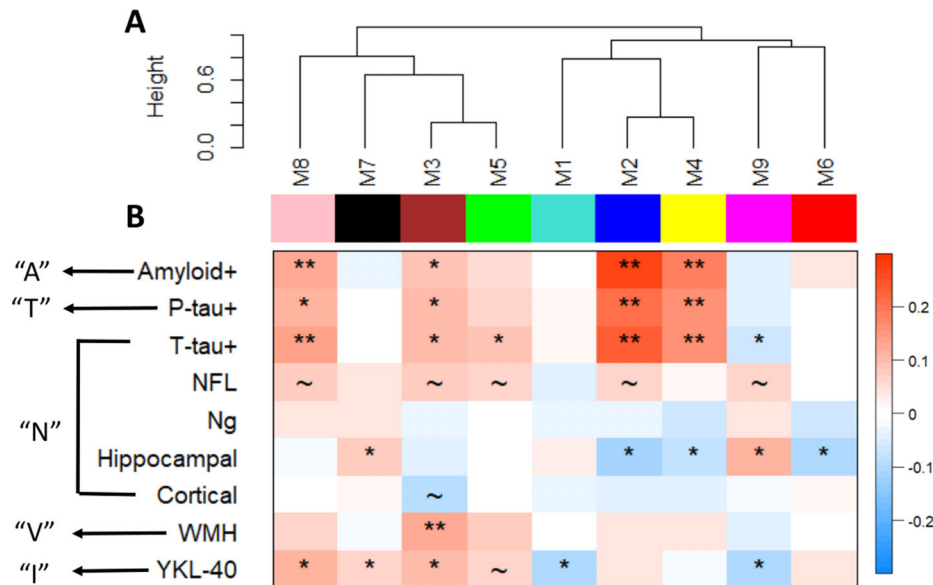


**FIGURE 2** Protein modules correlating to Alzheimer's disease (AD) pathology markers. A, Weighted gene correlation network analysis (WGCNA) of the plasma proteome. This algorithm generated nine modules (M) of co-expressed proteins. Modules are clustered in the network dendrogram based on their relatedness. B, Analysis of the association of module with AD pathology markers. \* and \*\* denote significant correlations  $P < .05$  and  $P < .001$  after false discovery rate (FDR) correction respectively. ~ indicates corrected  $P$  value tend to be significant,  $.05 < \text{corrected } P \text{ value} < .1$ . “A,” amyloid; “T,” tau; “N,” neurodegeneration; “V,” vascular; “I,” inflammation; +, abnormality; P-tau, phosphorylated tau; T-tau, total tau; NFL, neurofilament light chain; Ng, neurogranin; WMH, white matter hyperintensity

expression patterns. We further investigated the biological significance of proteins in each module and found that the modules were enriched with various pathways after FDR correction (Table S2 in supporting information), such as the metabolic pathways (M1 and M4), cytokine–cytokine receptor interaction (M2 and M3), PI3K–Akt signaling pathway (M5), transcriptional misregulation in cancer (M6), and complement and coagulation cascades (M7).

We then assessed the module correlations to the AD pathology markers (Figure 2B). We used  $A\beta$  as “A”; CSF p-tau levels as a biomarker of tau (“T”); CSF t-tau, NFL, Ng, and structural atrophy on MRI (hippocampal volume and cortical thickness) as biomarkers of “N”; WMH volume as a biomarker for vascular disease burden (“V”); and CSF YKL-40 as a biomarker of inflammation (“I”).

Overall, four modules (M2 blue, M3 brown, M4 yellow, and M8 pink) had positive correlations with both “A” amyloid and “T” p-tau pathology after FDR correction. For “N,” five modules (M2 blue, M3 brown, M4 yellow, M5 green, and M8 pink) had a positive correlation, while the M9 magenta module had a negative correlation with CSF t-tau. Of these, three (M2 blue, M4 yellow, and M9 magenta) were consistent in their direction of change and reached statistical significance for hippocampal volume (Figure 2B). Although none of the modules reached statistical significance with CSF NFL and Ng or cortical thickness, the association between five modules (M2 blue, M3 brown, M5 green, M8 pink, and M9 magenta) and NFL tended to be significant (corrected  $P$  values = .07 for all five modules). The same tendency was also observed between M3 brown and cortical thickness (corrected  $P$  value = .06; Figure 2B). For “V” and “I,” one and five modules were associated with WMH and YKL-40, respectively (Figure 2B).

### 3.3 | Correlation of protein networks with the ATN framework

We first assessed correlations for each module with the ATN framework where “A,” “T,” and “N” were determined by amyloid, CSF p-tau, and t-tau measurement, respectively. We dichotomized the relevant biomarkers as normal or abnormal and categorized each individual into one of four groups: A–T–N– (no pathology,  $n = 273$ ), A+TN– (amyloid pathology,  $n = 115$ ), A+TN+ (AD pathology,  $n = 383$ ), and A–TN+ (SNAP,  $n = 89$ ). We then assessed the correlation of these ATN profiles with each module eigenprotein. We found that four modules (M2 blue, M3 brown, M4 yellow, and M8 pink) showed a significant difference across ATN profiles (Figure 3A–D). They could be divided into two groups: (1) those influenced by amyloid pathology (A+); for example, M2 blue and M4 yellow modules showed significant difference between A–TN– and A+TN– as well as between A+TN+ and A–TN+ profiles. (2) Those influenced by tau pathology and neurodegeneration (TN+); for example, M2 blue, M3 brown, and M8 pink showed significant increase in A+TN+ compared to A+TN– profile (Figure 3A–D). We also checked the module correlations to the ATN framework in CTL only ( $n = 372$ ). Of the four modules, two (M2 blue and M4 yellow) had a significant increase in individuals with A+TN+ and A+TN– profiles compared to A–TN– (Figure S1B and C in supporting information).

We then used logistic regression to identify differential expressed proteins between different ATN profiles and A–TN– (using t-tau as “N”), adjusting for age and APOE  $\epsilon 4$  genotype. Comparing amyloid-only pathology (A+TN–) to no pathology (A–TN–), we found that 154 proteins reached statistical significance ( $P < .05$ ) but none survived FDR

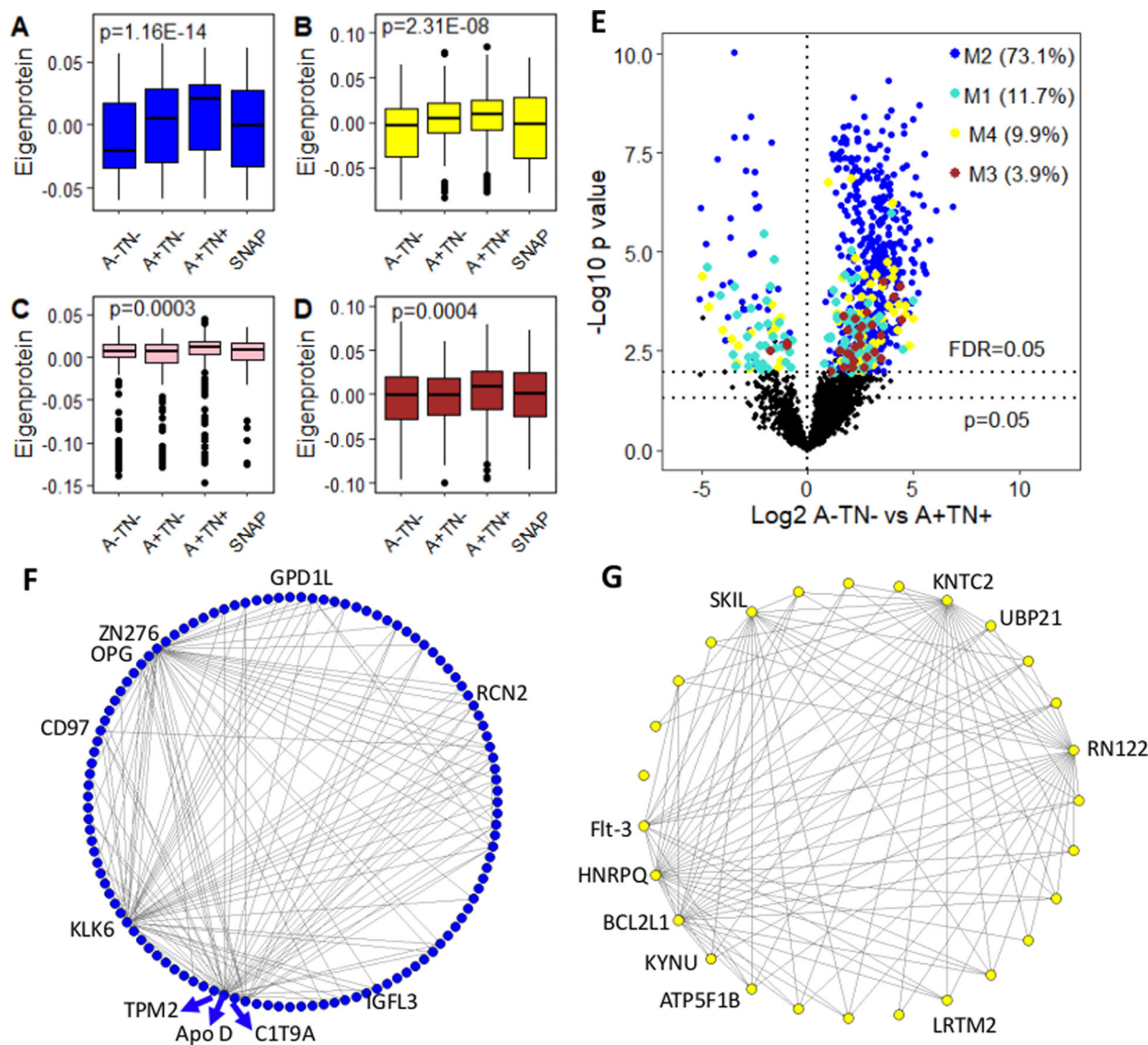


**FIGURE 3** Protein modules correlate to amyloid/tau/neurodegeneration (ATN) profile. A-D, The correlation of module profiles with the ATN framework, using t-tau as “N.” E, Volcano plot displaying all proteins differentially expressed between A-TN- and A+TN+ individuals. Proteins passing FDR ( $q < 0.05$ ) are noted in the same color as the module color. F and G, Top 10 hub proteins within M2 blue and M4 yellow module respectively. SNAP, suspected non-Alzheimer’s pathology; M, module; FDR, false discovery rate

correction ( $q < 0.05$ ; Figure S2A in supporting information). Equally, no proteins passed FDR comparing A-TN+ (SNAP) to no pathology (A-TN-; Figure S2B). However, in contrast, 776 survived FDR comparing AD pathology (A+TN+) to no pathology (A-TN-). As demonstrated in the volcano plot of Figure 3E, the majority of DE proteins were in the M2 blue module (73.1%), followed by M1 turquoise (11.7%), M4 yellow (9.9%), and M3 brown (3.9%) modules, indicating consistency across differential expression analysis and co-expression network analysis. Pathway enrichment analysis further showed that DE proteins were enriched in nine pathways such as AD pathway (Table S3 in supporting information).

In protein co-expression networks, hub proteins are likely important proteins because they are highly correlated with other proteins in the module. We sought to determine whether proteins DE in A+TN+ individuals were also hub proteins in the co-expression networks. We

focused on the two modules (M2 blue and M4 yellow) that showed a significant difference across ATN profiles in both all samples and CTL only. These two modules had 142 hub proteins (115 from M2 blue and 27 from M4 yellow), of which 141 proteins (99.3%) were DE in A+TN+ individuals, further indicating the consistency between protein co-expression network analysis and proteome wide differential analysis. Figure 3F and G showed the top 10 hub proteins within the M2 blue and M4 yellow module, respectively (Table S4 in supporting information).

As we had multiple measures that have been used as markers of neurodegeneration or “N,” we explored the relationship of each with the protein networks. Of the four modules (M2 blue, M3 brown, M4 yellow, and M8 pink) significantly increased in A+TN+ when t-tau was used as “N” (Figure 3A-D), three and two remained significant when NfL and hippocampal volume were used as “N,” respectively

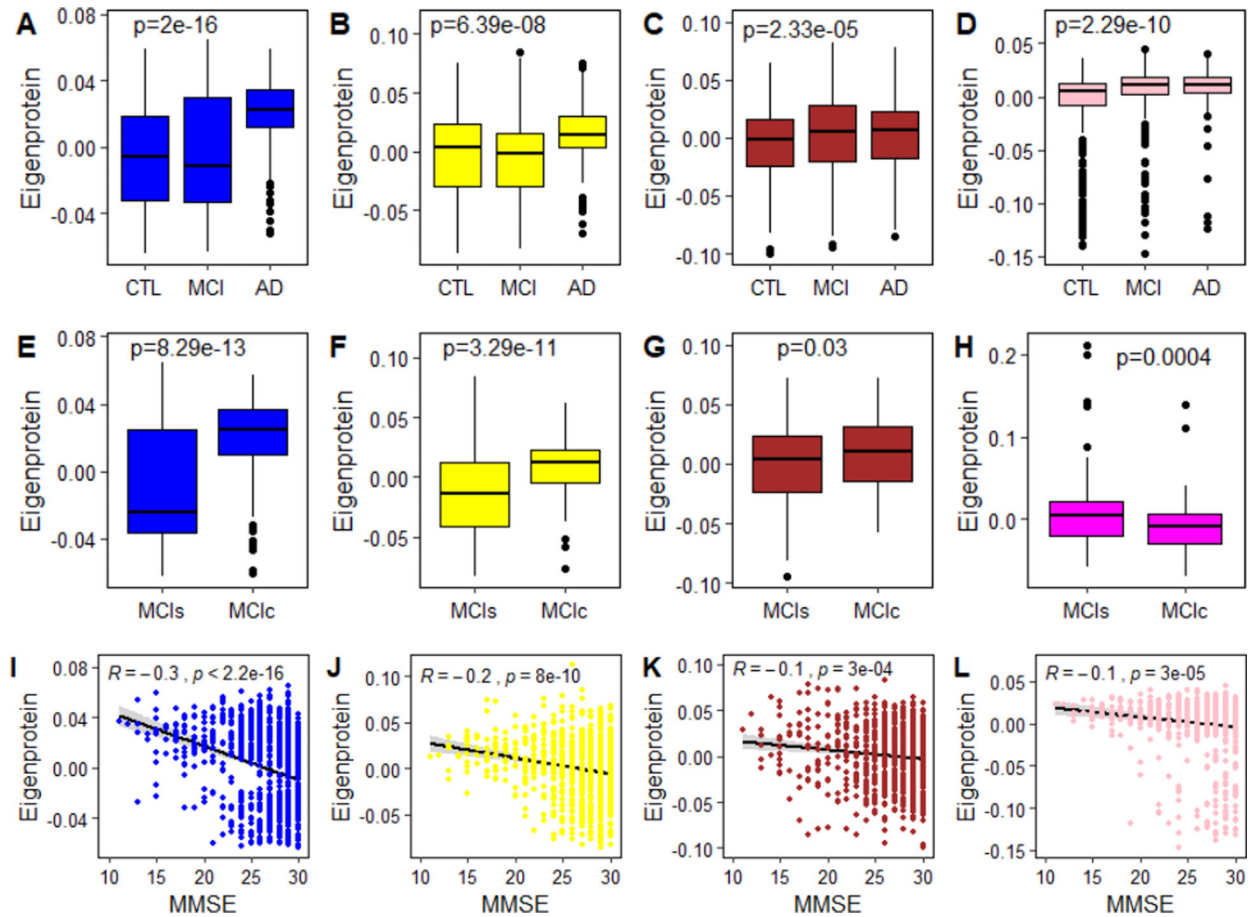


**FIGURE 4** Protein module associations with Alzheimer's disease (AD) diagnosis (A-D), MCI conversion (E-H), and correlations with cognitive status (I-L). CTL, control; MCI, mild cognitive impairment; MCIc, MCI converters; MCIs, stable MCI or MCI non-converted to AD; MMSE, Mini-Mental State Examination

(Figure S3A-C and Figure S3E and F in supporting information). From differential expressed proteins analysis (A+TN+ vs. A-TN-), we found 151 and 974 proteins passed FDR when NfL and hippocampal volume were used as "N," respectively (Figure S4A and B in supporting information). One hundred thirty-four proteins were overlapping across three different "N" markers (Figure S4C), which was significantly higher than expected by chance alone ( $P < .001$ ), indicating the similarity of protein profile across three "N" markers. Pathway enrichment of DE proteins revealed no pathways passed FDR correction when using NfL as "N." In contrast, 42 pathways were enriched using hippocampal volume as "N," among which 9 were overlapping with those obtained using t-tau as "N" (Table S3). Considering that more samples had CSF t-tau ( $n = 880$ ) measurement than NfL ( $n = 643$ ) or MRI ( $n = 633$ ) measurements, we therefore used CSF t-tau as biomarkers of neurodegeneration ("N") for the following analysis.

### 3.4 | Correlation of protein networks with AD diagnosis, MCI conversion, and MMSE score

We further investigated the module correlations to clinical measures including AD diagnosis, MCI conversion, and MMSE score. The M2

blue, M3 brown, M4 yellow, and M8 pink modules showed significant increase in AD compared to MCI and controls (Figure 4A-D). The eigenproteins for three modules (M2 blue, M3 brown, M4 yellow) also increased between MCI converters (MCIc,  $n = 103$ ) and MCI non-converters (MCIs,  $n = 223$ ) (Figure 4E-G). In contrast, M9 magenta decreased in MCI converters (Figure 4H). Furthermore, all four modules (M2 blue, M3 brown, M4 yellow, and M8 pink) were negatively correlated with the MMSE score (Figure 4I-L). These results are in concordance with ATN correlations as these four modules showed a strong increase in A+TN+ individuals.

### 3.5 | Multiprotein classifier of AD diagnosis and MCI conversion

Having demonstrated the correlation of protein networks with AD clinical groups, we then sought to find a minimal signal from the SOMAScan assay data that might serve as a biomarker for clinical AD diagnosis. To do this we built machine learning classifiers with 10-fold cross-validation to identify the optimal multivariate signatures that differentiated between AD and CTL. We first used demographic variables (age, sex, and education) with APOE  $\epsilon 4$  genotype as input features



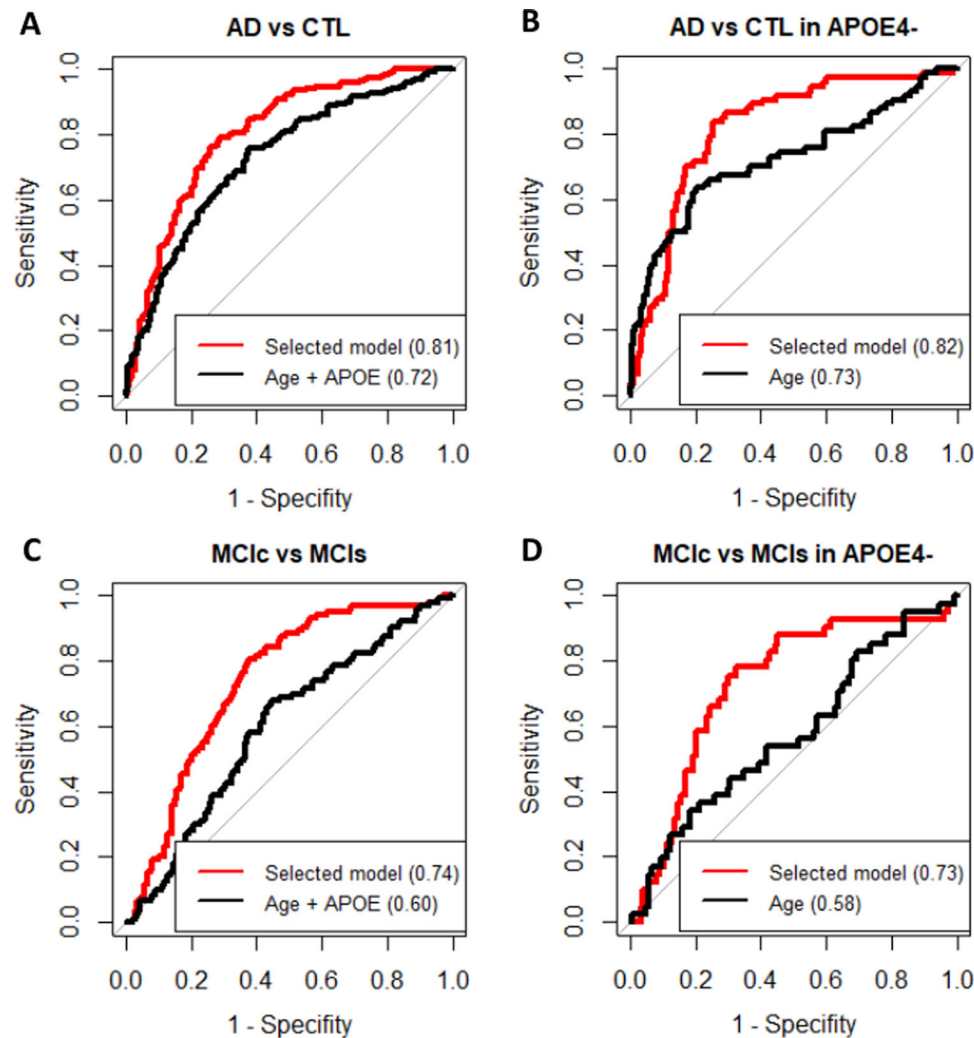


**FIGURE 5** Receiver operating characteristic (ROC) curves of models distinguishing Alzheimer's disease (AD) from controls in (A) whole group and (B) APOE  $\epsilon 4$  genotype negative group as well as mild cognitive impairment (MCI) conversion in (C) whole group and (D) APOE  $\epsilon 4$  genotype negative group. APOE, apolipoprotein E; CTL, control; MCIc, MCI converted to AD; MCIs, stable MCI or MCI non-converted to AD

to predict AD diagnosis and found that a combination of age and APOE  $\epsilon 4$  achieved the highest predictive value with an AUC (area under the curve) of 0.72 with 95% confidence intervals (CI; 0.69, 0.78; Figure 5A). Then, we added 142 hub proteins of M2 blue and M4 yellow modules and identified a panel of eight features achieved the highest predictive value with an AUC of 0.81 (95% CI [0.78, 0.85]; Figure 5A). The input features automatically selected by the classifier were APOE  $\epsilon 4$  genotype and seven proteins (Table S5 in supporting information). We further performed such comparison in the APOE  $\epsilon 4$  negative group and found that a model containing nine proteins (Table S5) best discriminated AD from controls with an AUC of 0.82 (95% CI [0.80, 0.89]), which was higher than age alone (AUC = 0.73, 95% CI [0.66, 0.80]; Figure 5B).

Based on the same approach, we developed a model containing three proteins (Table S5) that best discriminated MCIc from MCIs. The diagnostic accuracy was higher (AUC = 0.74, 95% CI [0.71, 0.81]) compared to those obtained using age and APOE  $\epsilon 4$  genotype alone (AUC = 0.60, 95% CI [0.56, 0.68]; Figure 5C). Higher accuracy was also

observed in the APOE  $\epsilon 4$  negative group using proteins (AUC = 0.73, 95% CI [0.68, 0.85]) compared to age alone (AUC = 0.58, 95% CI [0.51, 0.71]; Figure 5D).

### 3.6 | Replication of several proteins using ELISA and Luminex xMAP

We also measured 25 proteins in the same cohort using targeted approaches including individual assay (ELISA) and multiplexed platforms such as Luminex xMAP (Figure 1B).<sup>15</sup> Overall, 20 of these proteins overlapped with the SOMAScan array. Of these, eight proteins were DE in A-TN- relative to A+TN+. Four were both consistent in direction of change compared to the SOMAScan assay and reached statistical significance: ficolin 2 (FCN2) (Figure 6A and E), plasminogen activator inhibitor 1 (PAI-1), C-reactive protein (CRP), and vascular cell adhesion protein 1 (sVCAM1; Figure S5A-F in supporting information). In terms of AD diagnosis, two proteins were differently

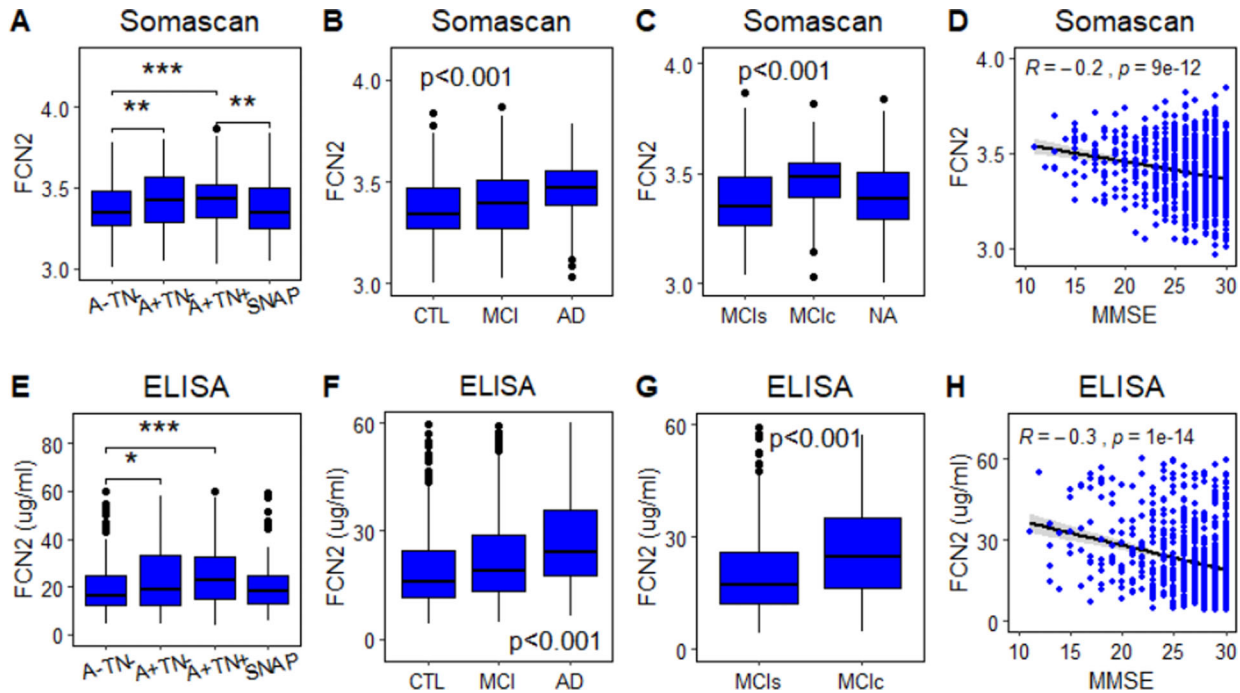


**FIGURE 6** Correlation of ficolin-2 (FCN2) with amyloid/tau/neurodegeneration (ATN), Alzheimer's disease (AD) diagnosis, mild cognitive impairment (MCI) conversion, and MMSE form SOMAscan (A-D) and targeted approaches (E-H). CTL, control; MCI, mild cognitive impairment; MCIC, MCI converters; MCIs, stable MCI or MCI non-converted to AD; MMSE, Mini-Mental State Examination; SNAP, suspected non-Alzheimer's pathology;

altered between AD and CTL from both approaches. They were FCN2 (Figure 6B and F) and PAI-1 (Figure S6A and B in supporting information). FCN2 also showed consistent strong increases in MCIC compared to MCIs from both approaches (Figure 6C and G). In addition, two proteins showed consistent significant relation with MMSE. Of these, FCN2 had a negative correlation with MMSE (Figure 6D and H) and PAI-1 had positive correlations with MMSE (Figure S6C and D).

## 4 | DISCUSSION

In this study, we measured plasma proteins from 972 subjects (372 CTL, 409 MCI, and 191 AD) using both capture array proteomics (SOMAscan) and targeted assays (ELISA and Luminex). For SOMAscan data, we performed both proteome-wide differential analysis and protein co-expression network analysis to gain insights into changes in individual proteins as well as networks of proteins relating to the ATN framework. We found consistent results through both approaches. Another notable finding is that the relation between proteins and "N" varied across different neurodegeneration markers, suggesting that ATN variants are not interchangeable from the perspective of plasma protein profiles. When using t-tau as "N," we found four modules were related to the ATN framework in all subjects, among which two (M2 blue and M4 yellow) were also related to the ATN framework in the cognitively normal group. Furthermore, these four modules were also associated with AD clinical diagnosis and MMSE score. Using hub proteins along with age and APOE  $\epsilon$ 4 genotype discriminated AD from con-

trols with an AUC of 0.81 and MCIC from MCIs with an AUC of 0.74. From targeted protein analysis, we replicated the relations of four proteins with the ATN framework and AD clinical diagnosis.

The increasing recognition that a broad spectrum of pathologies contribute to AD has highlighted the urgent need for biomarkers that more comprehensively reflect the complex mechanisms underlying this disease.<sup>19,20</sup> However, current methods of measuring AD pathology markers are challenging because of their invasiveness, high cost, and limited availability. To address this challenge, we applied an integrative proteomics approach to identify plasma markers linked to a variety of AD pathology markers including "A," "T," "N," "V," and "I." We found four modules had positive correlations with both "A" amyloid and "T" p-tau181 pathology. At the time of conducting the study, CSF p-tau 181 was the optimal assay for estimation of pathological tau in biofluids. The proteins within these four modules were enriched in various pathways that have been reported to be associated with AD such as the Ras signaling pathway,<sup>21</sup> MAPK signaling pathway<sup>22</sup> and JAK-STAT signaling pathway,<sup>23</sup> further demonstrating the relatedness of these proteins with AD. Five modules were found to be associated with the "I" marker YKL-40, among which three modules (M1 turquoise, M3 brown, and M7 black) were enriched in inflammatory response pathways such as cytokine-cytokine receptor interaction and complement and coagulation cascades (Table S2).

The discrepancy of the association between modules and different "N" markers is noteworthy. As shown in Figure 2, six modules were significantly related to CSF t-tau, while none of them reached statistical significance with CSF NFL or Ng. A distinct difference was also observed when using t-tau, NFL, and hippocampal volume as "N" for

the ATN framework from both protein co-expression network analysis and differential analysis. For example, of the four modules associated with the ATN framework when using t-tau as "N," only three and two remain significant when using NFL and hippocampal volume as "N," respectively. From differentially expression analysis, 776 and 974 proteins were DE in A+TN+ when t-tau and hippocampal volume were used as "N" respectively, while only 151 proteins remained significant when NFL was used. Our results therefore indicate that ATN variants are not interchangeable from the perspective of plasma protein profiles. This finding is consistent with a recent study showing that different ATN variants are not interchangeable from the perspective of clinical stage.<sup>24</sup> Therefore, although different markers could be used as "N," their underlying mechanism and association with clinical outcomes are different, suggesting care needs to be taken in using these different markers when applying the ATN classification framework.

When using t-tau as "N," we found consistent results through proteome-wide differential analysis and protein co-expression network analysis related to the ATN framework. For instance, ~87% of the differentially expressed proteins in A+TN+ individuals were in three ATN-related modules (M2 blue, M3 brown, and M4 yellow). Furthermore, more than 99% of the hub proteins within two modules (M2 blue and M4 yellow) were DE proteins in A+TN+ individuals. Of these hub proteins (Table S4), many have been reported being associated with AD, such as the apolipoprotein proteins (Apo B and D,<sup>25,26</sup> complement component C6 and C7,<sup>27,28</sup> kallikrein (KLK6 and KLK12),<sup>29,30</sup> mitochondrial-related proteins (COX42 and ATP5F1B),<sup>31,32</sup> and so on. As these hub proteins are in M2 blue and M4 yellow modules, which were related to the ATN framework in individuals with no cognitive impairment, namely in the pre-clinical stage, it provides implications that they are tractable targets for further mechanistic studies of AD pathology, particularly in preclinical stages of AD.

As expected, four ATN framework related modules were also highly expressed in samples from people with AD and negatively associated with MMSE score. Using hub proteins within M2 blue and M4 yellow modules, we identified a panel of proteins that can identify study participants with AD as well as predict MCI conversion. For those 14 selected proteins (Table S5), we further compared the relations between these proteins with APOE  $\epsilon$ 4 genotype and age. Results showed that all of them were significantly DE between APOE  $\epsilon$ 4 positive and negative groups. Eight of them were significantly associated with age (Table S6 in supporting information). Comparing different diagnostic groups, we found that the majority of the proteins remained significantly DE between APOE  $\epsilon$ 4 positive and negative individuals within MCI and CTL groups, but not in AD patients (Table S6). This might be due to the small sample size of AD patients ( $n = 191$ ). These signatures, generated from proteins, had considerably more accuracy than age and APOE  $\epsilon$ 4 alone, the two biggest risk factors of AD. Furthermore, we found that the predictive value of these protein signatures was retained also in APOE  $\epsilon$ 4 negative groups. This is important because the proportion of APOE  $\epsilon$ 4 carriers in the general population is low (10% to 20%)<sup>33</sup> and therefore relying on APOE  $\epsilon$ 4 to enhance recruitment to clinical trials is problematic. The results that we report here raise the possibility of prescreening in large num-

bers of individuals, regardless of APOE  $\epsilon$ 4 genotype, as part of trials recruitment to speed the development of therapeutic interventions for AD.

From the targeted protein analysis, we replicated the relationships of four proteins (FCN2, PAI-1, CRP, and sVCAM1) with the ATN framework and with AD clinical diagnosis. Our initial discovery-phase studies demonstrated that these four proteins have a relationship with AD and its pathology.<sup>34</sup> Furthermore, these four biomarker candidates are also biologically relevant to the disease process. For example, FCN2 and mannose-binding lectin (MBL) are both activators of the lectin complement pathway<sup>35</sup> and CSF MBL levels have been shown to be reduced in AD.<sup>36</sup> PAI-1 is involved in A $\beta$  accumulation processes and knocking out the PAI-1 gene or adding PAI-1 inhibitors dramatically reduces A $\beta$  burden in the brain of APP/PS1 mice.<sup>37,38</sup> CRP inhibited A $\beta$ 40 in a Ca<sup>2+</sup>-independent manner and interacted with aggregated A $\beta$ 40 on the fibril-forming pathway.<sup>39</sup> sVCAM1, cell adhesion molecules, serve as signal transducers that influence the progression of neuroinflammation.<sup>40</sup> Our replication further demonstrates that these proteins are involved in AD pathology pathways and could be promising targets for future mechanistic studies.

There are three limitations to our study. First, this is an association study and thus it precludes causal inference. Further analysis such as implementing Mendelian randomization to integrate genomics and proteomics could help to find proteins causing AD pathology. Second, the EMIF cohort was designed to be typical of participants who had high ratios of amyloid pathology and APOE  $\epsilon$ 4 carriers. Therefore they are not necessarily representative of the broader community as would be found in epidemiologically derived samples. Thus the present results should not be generalized to community-based populations without further investigation. Third, this is a cross-sectional study and longitudinal studies are required to determine the role and mechanisms of nominated proteins in AD initiation and progression.

Despite this, our study is the largest plasma proteomic study of various AD pathology markers, particularly the ATN framework, to our knowledge. By applying both proteome-wide differential analysis and protein co-expression network analysis, our findings offer new insights into changes in individual proteins and protein networks linked to AD pathology markers as well as the ATN framework in poorly understood preclinical stages of AD. Those nominated hub proteins are tractable targets for further mechanistic studies of AD pathology. Our findings also suggest that the relationships between plasma proteins and "N" are dependent on the choice of neurodegeneration marker, indicating that the ATN variants are not interchangeable. In addition, it confirms that highly multiplexed assays are able to predict the presence of AD pathology as measured in the ATN framework as well as clinical diagnosis. This can be potentially applied as a prescreen to preselect patients for further selection procedures for clinical trials, thus reducing the cost incurred to clinical trials by screen failure.

## ACKNOWLEDGMENTS

This research was conducted as part of the EMIF-AD MBD project, which has received support from the Innovative Medicines Initiative Joint Undertaking under EMIF grant agreement n° 115372,

resources of which are composed of financial contribution from the European Union's Seventh Framework Programme (FP7/2007-2013) and EFPIA companies' in-kind contribution. The DESCRIPA study was funded by the European Commission within the 5th framework program (QLRT-2001-2455). The EDAR study was funded by the European Commission within the 5th framework program (contract # 37670). The Leuven cohort was funded by the Stichting voor Alzheimer Onderzoek (grant numbers #11020, #13007, and #15005). RV is a senior clinical investigator of the Flemish Research Foundation (FWO). The San Sebastian GAP study is partially funded by the Department of Health of the Basque Government (allocation 17.0.1.08.12.0000.2.454.01.41142.001.H). We acknowledge the contribution of the personnel of the Genomic Service Facility at the VIB-U Antwerp Center for Molecular Neurology. The research at VIB-CMN is funded in part by the University of Antwerp Research Fund. HZ is a Wallenberg Scholar supported by grants from the Swedish Research Council (#2018-02532); the European Research Council (#681712); Swedish State Support for Clinical Research (#ALFGBG-720931); the Alzheimer Drug Discovery Foundation (ADDF), USA (#201809-2016862); and the UK Dementia Research Institute at UCL. FB is supported by the NIHR biomedical research center at UCLH.

#### ETHICS STATEMENT

Written informed consent was obtained from all participants before inclusion in the study. The medical ethics committee at each site approved the study.

#### CONFLICTS OF INTEREST

Simon Lovstone is named as an inventor on biomarker intellectual property protected by Proteome Sciences and King's College London unrelated to the current study and within the past 5 years has advised for Optum labs, Merck, SomaLogic and been the recipient of funding from AstraZeneca and other companies via the IMI funding scheme. Henrik Zetterberg has served on scientific advisory boards for Denali, Roche Diagnostics, Wave, Samumed, Siemens Healthineers, Pinteon Therapeutics, and CogRx; has given lectures in symposia sponsored by Fujirebio, Alzecure, and Biogen; and is a co-founder of Brain Biomarker Solutions in Gothenburg AB (BBS), which is a part of the GU Ventures Incubator Program (all unrelated to this study). Jose L. Molinuevo has served on scientific advisory boards for Eli Lilly, Roche Diagnostics, Roche, Biogen, Lundbeck, Novartis, IBL, Axovant, Oryzon, and Merck (all unrelated to this study). Alberto Lleo has served on scientific advisory boards of Fujirebio Europe, Eli Lilly, Novartis, Nutricia, and Otsuka and is the inventor of a patent on synaptic markers in CSF (all unrelated to this study). Lutz Frolich has received research funding, consultancy fees, or speech honoraria from Allergan, Avid-Eli Lilly, Avanir, Avraham Pharmaceuticals, Axon Neuroscience, Axovant, Biogen, Boehringer Ingelheim, Eisai, Functional Neuromodulation, GE Health Care, Lundbeck, MerckSharpe&Dohme, Novartis, Pfizer, Pirmal Imaging, Roche, and Schwabe Pharma. Julius Popp has served on scientific advisory boards of Fujirebio Europe, Eli Lilly, and Nestlé Institute of Health Sciences, all unrelated to this study. Sebastiaan

Engelborghs has received unrestricted research grants from Janssen Pharmaceutica and ADx Neurosciences and has served on scientific advisory boards of Biogen, Eisai, Novartis, Nutricia/Danone, all unrelated to this study. Charlotte E. Teunissen advises Roche; received research reagents from ADxNeurosciences and Euroimmun; and has received contract research and grants from AxonNeurosciences, Biogen, Boehringer, Brainstorm Therapeutics, Celgene, EIP Pharma, Eisai, Janssen prevention center, Roche, Toyama, and Vivoryon.

#### DATA AVAILABILITY STATEMENT

The datasets generated and analysed during the current study are available from the EMIF-AD Catalogue via submitted research proposals that have to be approved by the data-owners from each parent cohort.

#### REFERENCES

- Lane CA, Hardy J, Schott JM. Alzheimer's disease. *Eur J Neurol*. 2018;25:59-70.
- Schöll M, Maass A, Mattsson N, et al. Biomarkers for tau pathology. *Mol Cell Neurosci*. 2019;97:18-33.
- Cohen AD, Landau SM, Snitz BE, Klunk WE, Blennow K, Zetterberg H. Fluid and PET biomarkers for amyloid pathology in Alzheimer's disease. *Mol Cell Neurosci*. 2018;97:3-17.
- Jack CR, Jr., Bennett DA, Blennow K, et al. NIA-AA research framework: toward a biological definition of Alzheimer's disease. *Alzheimers Dement*. 2018;14:535-562.
- Zetterberg H, Skillback T, Mattsson N, et al. Association of cerebrospinal fluid neurofilament light concentration with Alzheimer disease progression. *JAMA Neurol*. 2016;73:60-67.
- Portelius E, Zetterberg H, Skillback T, et al. Cerebrospinal fluid neurogranin: relation to cognition and neurodegeneration in Alzheimer's disease. *Brain*. 2015;138:3373-3385.
- Lista S, Faltraco F, Prvulovic D, Hampel H. Blood and plasma-based proteomic biomarker research in Alzheimer's disease. *Prog Neurobiol*. 2013;101-102:1-17.
- de Almeida SM, Shumaker SD, LeBlanc SK, et al. Incidence of post-dural puncture headache in research volunteers. *Headache*. 2011;51:1503-1510.
- Hye A, Lynham S, Thambisetty M, et al. Proteome-based plasma biomarkers for Alzheimer's disease. *Brain*. 2006;129:3042-3050.
- Thambisetty M, Simmons A, Velayudhan L, et al. Association of plasma clusterin concentration with severity, pathology, and progression in Alzheimer disease. *Arch Gen Psychiatry*. 2010;67:739-748.
- Kiddle SJ, Sattlecker M, Proitsi P, et al. Candidate blood proteome markers of Alzheimer's disease onset and progression: a systematic review and replication study. *J Alzheimers Dis*. 2014;38:515-531.
- Sattlecker M, Kiddle SJ, Newhouse S, et al. Alzheimer's disease biomarker discovery using SOMAscan multiplexed protein technology. *Alzheimers Dement*. 2014;10:724-734.
- Baird AL, Westwood S, Lovestone S. Blood-based proteomic biomarkers of Alzheimer's disease pathology. *Front Neurol*. 2015;6:236.
- Shi L, Westwood S, Baird AL, et al. Discovery and validation of plasma proteomic biomarkers relating to brain amyloid burden by SOMAscan assay. *Alzheimer's Dement*. 2019;15:1478-1488.
- Westwood S, Baird AL, Anand SN, et al. Validation of plasma proteomic biomarkers relating to brain amyloid burden in the EMIF-Alzheimer's disease multimodal biomarker discovery cohort. *J Alzheimer's Dis*. 2020:1-13.
- Bos I, Vos S, Vandenberghe R, et al. The EMIF-AD multimodal biomarker discovery study: design, methods and cohort characteristics. *Alzheimers Res Ther*. 2018;10:64.



17. Gold L, Ayers D, Bertino J, et al. Aptamer-based multiplexed proteomic technology for biomarker discovery. *PLoS One* 2010;5:e15004.
18. Langfelder P, Horvath S. WGCNA: an R package for weighted correlation network analysis. *BMC Bioinformatics* 2008;9:559.
19. Lista S, Zetterberg H, O'Bryant SE, Blennow K, Hampel H. Evolving relevance of neuroproteomics in Alzheimer's disease. *Neuroproteomics*. Springer; 2017:101-115.
20. Castrillo JI, Lista S, Hampel H, Ritchie CW. Systems biology methods for Alzheimer's disease research toward molecular signatures, subtypes, and stages and precision medicine: application in cohort studies and trials. *Biomarkers Alzheimer's Dis. Drug Dev.* Springer; 2018:31-66.
21. Kirouac L, Rajic AJ, Cribbs DH, Padmanabhan J. Activation of Ras-ERK signaling and GSK-3 by amyloid precursor protein and amyloid beta facilitates neurodegeneration in Alzheimer's disease. *ENeuro*. 2017;4.
22. Ogishima S, Mizuno S, Kikuchi M, et al. A map of Alzheimer's disease-signaling pathways: a hope for drug target discovery. *Clin Pharmacol Ther.* 2013;93:399-401.
23. Nevado-Holgado AJ, Ribe E, Thei L, et al. Genetic and real-world clinical data, combined with empirical validation, nominate jak-stat signaling as a target for Alzheimer's disease therapeutic development. *Cells*. 2019;8:425.
24. Mattsson-Carlsson N, Leuzy A, Janelidze S, et al. The implications of different approaches to define AT (N) in Alzheimer disease. *Neurology*. 2020;94(21):e2233-e2244.
25. Kalman J, McConathy W, Araoz C, Kasa P, Lacko AG. Apolipoprotein D in the aging brain and in Alzheimer's dementia. *Neurol Res*. 2000;22:330-336.
26. Ishii M. Apolipoprotein B as a new link between cholesterol and Alzheimer disease. *JAMA Neurol*. 2019;76:751-753.
27. Crehan H, Hardy J, Pocock J. Microglia, Alzheimer's disease, and complement. *Int J Alzheimer's Dis*. 2012;2012:983640.
28. Shen Y, Yang L, Li R. What does complement do in Alzheimer's disease? Old molecules with new insights. *Transl Neurodegener*. 2013;2:1-11.
29. Zamolodchikov D, Chen Z-L, Conti BA, Renné T, Strickland S. Activation of the factor XII-driven contact system in Alzheimer's disease patient and mouse model plasma. *Proc Natl Acad Sci U S A*. 2015;112:4068-4073.
30. Goldhardt O, Warnhoff I, Yakushev I, et al. Kallikrein-related peptidases 6 and 10 are elevated in cerebrospinal fluid of patients with Alzheimer's disease and associated with CSF-TAU and FDG-PET. *Transl Neurodegener*. 2019;8:1-13.
31. Cardoso SM, Proença MT, Santos S, Santana I, Oliveira CR. Cytochrome c oxidase is decreased in Alzheimer's disease platelets. *Neurobiol Aging*. 2004;25:105-110.
32. Goldberg J, Currais A, Prior M, et al. The mitochondrial ATP synthase is a shared drug target for aging and dementia. *Aging Cell*. 2018;17:e12715.
33. Singh PP, Singh M, Mastana SS. APOE distribution in world populations with new data from India and the UK. *Ann Hum Biol*. 2006;33:279-308.
34. Shi L, Baird AL, Westwood S, et al. A decade of blood biomarkers for Alzheimer's disease research: an evolving field, improving study designs, and the challenge of replication. *J Alzheimers Dis*. 2018;62:1181-1198.
35. Fujita T, Matsushita M, Endo Y. The lectin-complement pathway—its role in innate immunity and evolution. *Immunol Rev*. 2004;198:185-202.
36. Lanzrein A-S, Jobst KA, Thiel S, et al. Mannan-binding lectin in human serum, cerebrospinal fluid and brain tissue and its role in Alzheimer's disease. *Neuroreport*. 1998;9:1491-1495.
37. Liu RM, van Groen T, Katre A, et al. Knockout of plasminogen activator inhibitor 1 gene reduces amyloid beta peptide burden in a mouse model of Alzheimer's disease. *Neurobiol Aging*. 2011;32:1079-1089.
38. Akhter H, Huang WT, van Groen T, Kuo HC, Miyata T, Liu RM. A small molecule inhibitor of plasminogen activator inhibitor-1 reduces brain amyloid- $\beta$  load and improves memory in an animal model of Alzheimer's disease. *J Alzheimers Dis*. 2018;64:447-457.
39. Ozawa D, Nomura R, Mangione PP, et al. Multifaceted anti-amyloidogenic and pro-amyloidogenic effects of C-reactive protein and serum amyloid P component in vitro. *Sci Rep*. 2016;6:29077.
40. Wennström M, Nielsen HM. Cell adhesion molecules in Alzheimer's disease. *Degener Neurol Neuromuscul Dis*. 2012;2:65-77.

## SUPPORTING INFORMATION

Additional supporting information may be found online in the Supporting Information section at the end of the article.

**How to cite this article:** Shi L, Winchester LM, Westwood S, et al. Replication study of plasma proteins relating to Alzheimer's pathology. *Alzheimer's Dement*. 2021;17:1452-1464. <https://doi.org/10.1002/alz.12322>